

Motor-dependent microtubule disassembly driven by tubulin tyrosination

Leticia Peris,^{1,2,4} Michael Wagenbach,⁵ Laurence Lafanechère,^{3,4,6} Jacques Brocard,^{1,2,4} Ayana T. Moore,⁵ Frank Kozielski,⁷ Didier Job,^{1,2,4} Linda Wordeman,⁵ and Annie Andrieux^{1,2,4}

¹Institut National de la Santé et de la Recherche Médicale Unité 836, Institut des Neurosciences de Grenoble, 38042 Grenoble, Cedex 9, France

²Groupe Physiopathologie du Cytosquelette and ³Criblage pour Molécules Bio-Actives, Institut de Recherches en Technologies et Sciences pour le Vivant, Direction des Sciences du Vivant, Commissariat à l'Énergie Atomique, 38054 Grenoble, Cedex 9, France

⁴Université Joseph Fourier, 38042 Grenoble, Cedex 9, France

⁵Department of Physiology and Biophysics, University of Washington, Seattle, WA 98195

⁶Centre National de la Recherche Scientifique, Unité Mixte de Recherche 5168, 38054 Grenoble, Cedex 9, France

⁷The Beatson Institute for Cancer Research, Glasgow G61 1BD, Scotland, UK

In cells, stable microtubules (MTs) are covalently modified by a carboxypeptidase, which removes the C-terminal Tyr residue of α -tubulin. The significance of this selective detyrosination of MTs is not understood. In this study, we report that tubulin detyrosination in fibroblasts inhibits MT disassembly. This inhibition is relieved by overexpression of the depolymerizing motor mitotic centromere-associated kinesin (MCAK). Conversely, suppression of MCAK expression prevents disassembly of normal tyrosinated MTs in fibroblasts. Detyrosination of MTs suppresses the activity of MCAK in vitro, apparently as the result of a

decreased affinity of the adenosine diphosphate (ADP)-inorganic phosphate- and ADP-bound forms of MCAK for the MT lattice. Detyrosination also impairs MT disassembly in neurons and inhibits the activity of the neuronal depolymerizing motor KIF2A in vitro. These results indicate that MT depolymerizing motors are directly inhibited by the detyrosination of tubulin, resulting in the stabilization of cellular MTs. Detyrosination of transiently stabilized MTs may give rise to persistent subpopulations of disassembly-resistant polymers to sustain subcellular cytoskeletal differentiation.

Introduction

Tubulin is subject to posttranslational modifications that principally affect the C terminus of its α subunit. In one of these modifications, the C-terminal Tyr residue of α -tubulin is cyclically removed from the peptide chain by a carboxypeptidase and then subsequently religated to the chain by tubulin Tyr ligase (TTL; Hammond et al., 2008). This cycle generates pools of tyrosinated and detyrosinated microtubules (MTs) in cells. As a rule, dynamic MTs are tyrosinated, whereas stable polymers are detyrosinated (Schulze et al., 1987). Detyrosination does not, per se, stabilize MTs (Khawaja et al., 1988). However, MT stabilization in cells induces MT detyrosination, which is thus considered as a consequence, not a cause, of MT stabilization (Webster et al., 1987).

In recent years, important functions of tubulin tyrosination have been discovered. Thus, TTL loss and the resulting

tubulin detyrosination confer selective advantage to cancer cells during tumor growth (Mialhe et al., 2001). TTL suppression in mice, which induces massive tubulin detyrosination, leads to lethal disorganization of neuronal circuits (Erck et al., 2005). Cells derived from TTL-deficient (TTL knockout [KO]) mice display morphogenetic and polarity anomalies (Peris et al., 2006). Tyrosination has turned out to be crucial for tubulin interaction with cytoskeletal-associated protein (CAP)-Gly plus end-tracking proteins (Badin-Larcon et al., 2004; Peris et al., 2006; Bieling et al., 2008; Steinmetz and Akhmanova, 2008), suggesting that the phenotypes observed after TTL suppression may arise from mislocalization of CAP-Gly proteins at detyrosinated MT plus ends. However, a mechanistic explanation for the long-recognized correlation between MT stability and tubulin tyrosination remains elusive. This prompted us to reexamine the relationship of tubulin tyrosination with

Correspondence to Leticia Peris: Leticia.peris@ujf-grenoble.fr; or Annie Andrieux: annie.andrieux@ujf-grenoble.fr

Abbreviations used in this paper: CAP, cytoskeletal-associated protein; CPA, carboxypeptidase A; KO, knockout; MCAK, mitotic centromere-associated kinesin; MEF, mouse embryonic fibroblast; MT, microtubule; Pi, inorganic phosphate; TIP, tip-interacting protein; TTL, tubulin Tyr ligase; WT, wild type.

© 2009 Peris et al. This article is distributed under the terms of an Attribution-Noncommercial-Share Alike-No Mirror Sites license for the first six months after the publication date (see <http://www.jcb.org/misc/terms.shtml>). After six months it is available under a Creative Commons License (Attribution-Noncommercial-Share Alike 3.0 Unported license, as described at <http://creativecommons.org/licenses/by-nc-sa/3.0/>).

MT dynamics using TTL KO cells in which MTs are extensively detyrosinated. We found that the tyrosination status of the MT had a profound effect on the MT-depolymerization activity of kinesin-13 family members.

Results and discussion

We initially observed decreased MT sensitivity to the depolymerizing drug nocodazole in TTL KO mouse embryonic fibroblasts (MEFs) compared with wild type (WT; Fig. 1 A), suggesting that MTs are stabilized in TTL KO MEFs. We have previously shown that the interaction of MTs with stabilizing factors such as structural microtubule-associated proteins or plus end-binding proteins is either unaffected or inhibited by tubulin detyrosination (Saoudi et al., 1995; Peris et al., 2006). Therefore, we hypothesized that in TTL KO cells, detyrosinated MTs might be a poor substrate for MT destabilizing factors such as the kinesin-13 protein mitotic centromere-associated kinesin (MCAK), which is an important depolymerizing motor in cycling cells (Newton et al., 2004; Mennella et al., 2005; Gupta et al., 2006; Manning et al., 2007; Ohi et al., 2007; Hedrick et al., 2008). Thus, MCAK overexpression should rescue the loss of dynamic MTs in TTL KO cells. Conversely, suppression of MCAK expression should prevent disassembly of normal tyrosinated MTs in fibroblasts. To test these possibilities, individual MT dynamics were monitored in WT or TTL KO MEFs. Cells were either untreated or transfected with MCAK cDNA or with MCAK siRNAs (Fig. S1 D shows MCAK depletion by siRNAs). MT behavior was scored close to the membrane in lamellipodial extensions.

In WT MEFs, most MTs depolymerized upon contact with the membrane (Fig. 1 B). In contrast, many MTs continued to grow tangential to the leading edge after touching the membrane in TTL KO MEFs (Fig. 1 B and Videos 1 and 2). The time spent by MTs close to the membrane (persistence time) was markedly increased in TTL KO MEFs as compared with WT MEFs. In TTL KO MEFs, MT persistence dropped dramatically after MCAK overexpression and became similar to that observed in WT MEFs (Fig. 1 C and Videos 3 and 4). MCAK depletion dramatically increased MT persistence time, which overran the observation time in >80% of the cases, in both genotypes (Videos 5 and 6).

We compared MT dynamic instability in WT and TTL KO (Fig. 1 D and Fig. S2). MTs in TTL KO MEFs displayed a higher frequency of rescues (threefold), an increase of the time spent growing (twofold), and a reduction of the time spent shrinking (twofold). In TTL KO cells, MCAK overexpression resulted in a decrease in the frequency of rescues (twofold) and a decrease in the time spent growing with a corresponding increase in the time spent pausing. MCAK depletion by siRNA increased the rescue frequency in WT cells (threefold) and increased the time spent pausing at the expense of the time spent shrinking in both genotypes. Interestingly, the two genotypes no longer exhibited significant differences in MT dynamics in the presence of MCAK siRNA.

These results indicate a reduction of MT disassembly and abnormal MT persistence after membrane contact in TTL KO cells.

MCAK overexpression partially rescued MT dynamic parameters in TTL KO MEFs, and MCAK suppression erased the inherent differences between the genotypes. These data are compatible with a simple model in which MCAK activity is impaired on detyrosinated MTs. Although no sizeable differences in MCAK expression were observed in TTL KO cells as compared with WT (Fig. S1, A–C), it is a formal possibility that MCAK activity could be affected indirectly.

To circumvent this, we assayed recombinant MCAK activity directly on the exposed MTs of the two MEF genotypes after cell lysis in a large volume of Triton X-100–based buffer to remove the cytosol. During lysis and further processing, MTs were stabilized with 2 μ M taxol to prevent spontaneous depolymerization. During the time course of experiments, in the absence of added exogenous MCAK, no detectable depolymerization of MTs occurred, indicating negligible endogenous MCAK activity in lysed cells (unpublished data). WT MEFs contained tyrosinated MTs, and TTL KO MEFs exhibited extensively detyrosinated MTs and variable amounts of tyrosinated tubulin originating from tubulin synthesis (Fig. 2 A; Peris et al., 2006). Fully detyrosinated MTs could be generated by treating WT lysed fibroblasts with carboxypeptidase A (CPA; WT + CPA; Fig. 2 A). WT and WT + CPA lysed MEFs contained similar quantities of MT polymer (Fig. 2, B and C). Lysed TTL KO fibroblasts also exhibited similar levels of MT polymer to that of WT fibroblasts (Fig. 2, B and C). After incubation with recombinant MCAK, WT MTs displayed extensive depolymerization. In contrast, CPA-treated WT MTs or MTs in TTL KO lysed fibroblasts were minimally affected by the addition of recombinant MCAK (Fig. 2, B and C). MT depolymerization was greater when TTL KO or WT + CPA MT arrays were incubated with a neck + motor domain mutant of MCAK instead of full-length MCAK (Fig. 2 C), but the extent of depolymerization was still less than that observed with WT MTs (Fig. 2 C). MT exposure to the motor domain alone, which is devoid of sizeable depolymerizing activity (Maney et al., 2001), did not induce any detectable depolymerization of any MT array (Fig. 2 C). These results strongly indicate a direct relationship between MT detyrosination and MCAK inhibition, which is evident even in the presence of the residual amounts of Tyr tubulin typically seen in TTL KO cells.

A possibility remained that tubulin detyrosination or CPA treatment inhibited MCAK by interfering with the interaction of the MTs with other cellular effector proteins. To control for this possibility, we assayed MCAK activity on MTs assembled with purified tyrosinated or detyrosinated tubulin (Fig. 3 A). MCAK activity on detyrosinated MTs was diminished compared with tyrosinated MTs, further supporting a direct relationship between MT tyrosination and MCAK activity (Fig. 3, B and C). We then used MT-binding assays to identify the point in the tubulin removal cycle that is affected by tubulin tyrosination. MCAK's apparent affinity for MTs is influenced by its nucleotide state (Helenius et al., 2006). Assays were run using the following nucleotides or nucleotide analogues: the nonhydrolyzable nucleotide analogue AMP-PNP (p[NH]ppA, adenosine 5'-[β , γ -imido]triphosphate), which mimics the ATP collision state; ADP-AlFx (ADP + aluminium + sodium fluoride), which

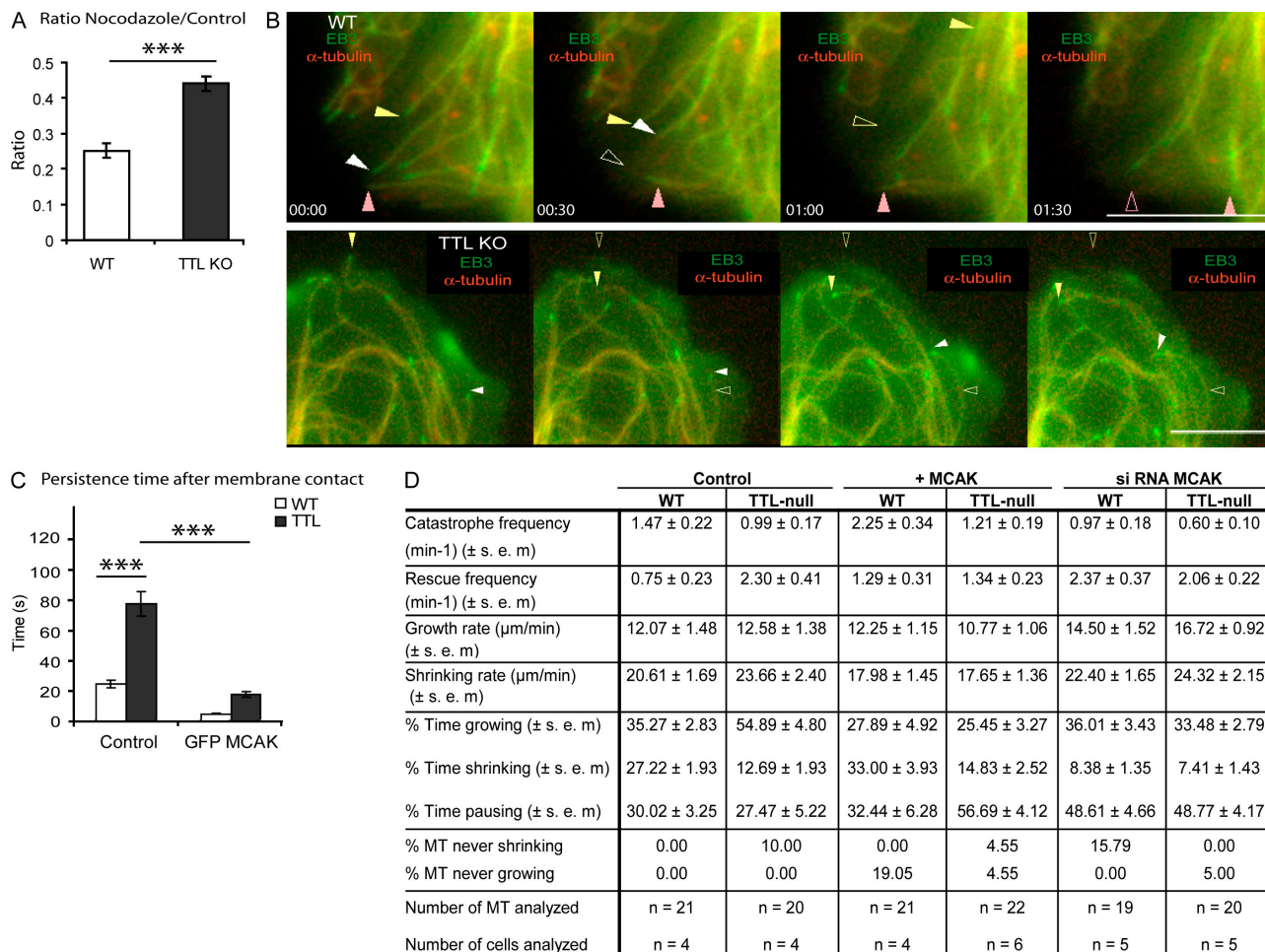


Figure 1. Impaired MT dynamics in TTL KO MEFs. (A) Analysis of nocodazole effects on WT or TTL KO MEFs. Data are expressed as the ratio of MT signals measured after nocodazole treatment versus control conditions (mean ± SEM). MT signals were estimated for a minimum of 39 MEFs from three independent experiments for each genotype and treatment condition. ***, $P < 0.001$ with a t test. (B) Video microscopy examination of MTs in WT or TTL KO MEFs expressing m-cherry α -tubulin and GFP-EB3 close to the leading edge of lamellipodial extensions. Colored, closed arrowheads indicate localization of the MT tip at different time points. Open arrowheads of the corresponding color indicate the initial MT tip localization. Most WT MTs underwent extensive depolymerization after membrane contact (white and yellow arrowheads). Some MTs followed the leading edge for a short period of time before depolymerization (pink arrowheads). Most TTL KO MTs continued to grow after membrane touch, running along the plasma membrane or even growing inward (white arrowheads). Occasionally, MTs seemed to push the membrane forward before disassembly, rescue, and regrowth (yellow arrowheads). Similar phenotypes were observed when MT ends were labeled with other TIPs or in experiments run with fluorescent tubulin alone (not depicted). (C) Measurement of the time spent by MTs exploring the area near the leading edge (persistence time). Experiments were run under control conditions or after cell transfection with either MCAK cDNA or MCAK siRNAs. At least 42 MTs were examined in each condition. With MCAK siRNAs, persistence times generally exceeded 100 s and overran the observation time (Videos 5 and 6). Results are shown in other conditions as mean values ± SEM. ***, $P < 0.001$ with a t test. (D) Analysis of MT dynamic instability. MTs whose growing plus tip was located within 10 μ m of the leading edge at time 0 were followed over time after various cell treatments, as indicated. Mean values ± SEM are shown. Statistically significant differences between WT and KO cells are described in Results and discussion; in all cases, p -values were < 0.01 with a Mann and Whitney U test. Bars, 10 μ m.

mimics the ATP transition state; ADP-vanadate, which mimics ADP–inorganic phosphate (Pi); and ADP (Fig. 4). By fluorescence microscopy, MCAK proteins yielded a punctuated decoration of MTs, with some aggregates in the background (Fig. 4 A), as previously observed (Moore and Wordeman, 2004). In quantitative experiments, the AMP-PNP-bound forms of GFP-MCAK or of the GFP neck + motor domain of MCAK associated to similar extents with tyrosinated or detyrosinated MTs (Fig. 4, B and C). In contrast, the ADP-AIFx–, ADP-vanadate–, and ADP-bound forms of full-length MCAK exhibited a diminished association with detyrosinated MTs compared with tyrosinated polymers (Fig. 4 B). The difference was maximal with the ADP-vanadate (Fig. 4 B). Similar results were observed

with the neck + motor domain of MCAK, although differences were smaller (Fig. 4 C). Thus, detyrosination seems to diminish the affinity of the MT lattice for the ADP-Pi– or ADP-bound forms of MCAK.

To test whether the inhibition of depolymerizing motors was unique to TTL KO MEFs, we assayed TTL KO neurons for similar resistance to MT disassembly. When WT or TTL KO neurons were exposed to nocodazole, only residual tubulin staining was detectable in the axons of WT neurons, whereas a persistent MT signal was evident in the axons of TTL-deficient neurons (Fig. 5, A–C). Axonal MT disassembly is largely dependent on the activity of KIF2A (Homma et al., 2003), a neuronal kinesin-13 in the same family as MCAK. KIF2A KO

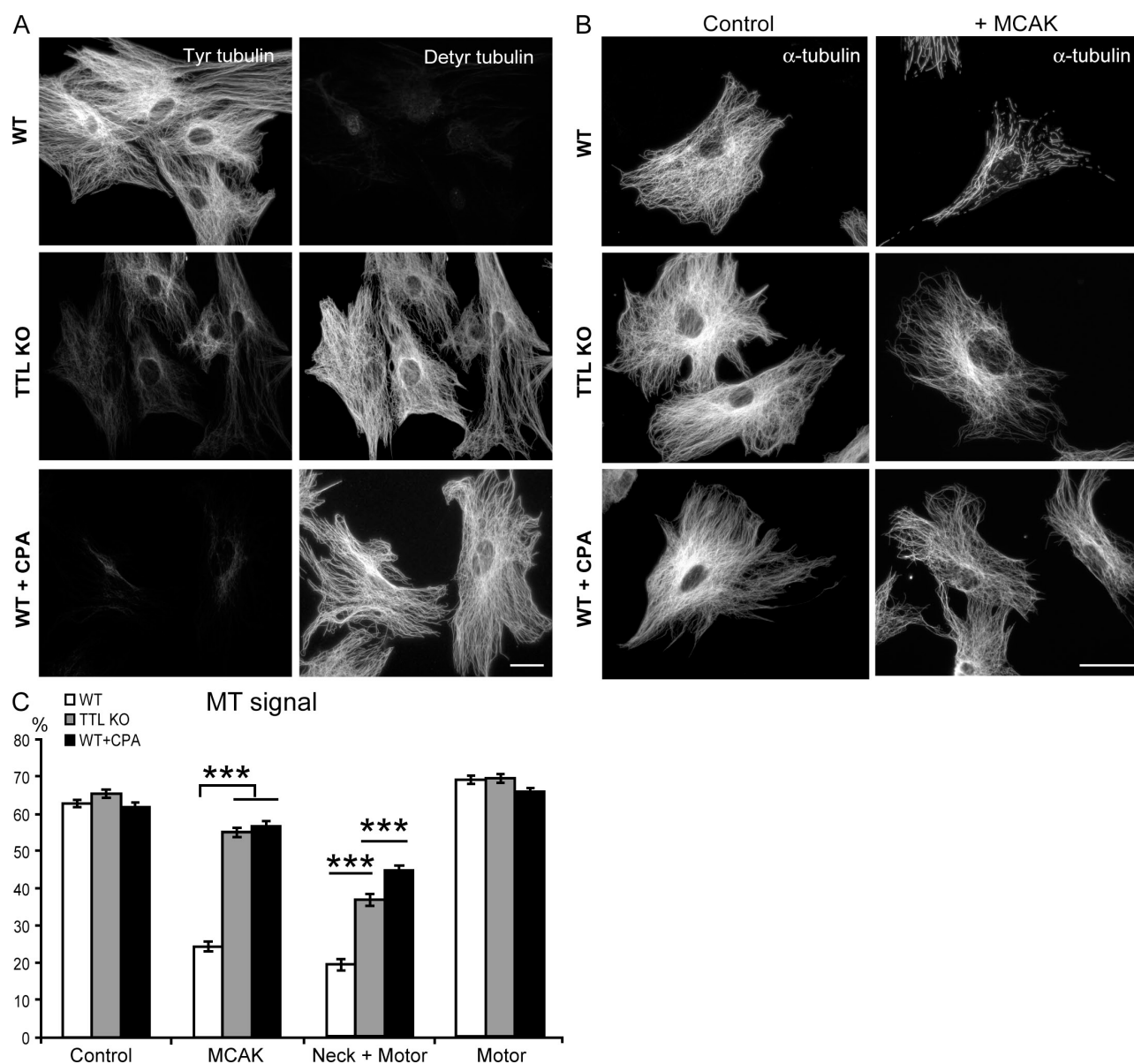


Figure 2. Depolymerizing activity of MCAK on tyrosinated or detyrosinated MTs in lysed cells. (A) MT tyrosination/detyrosination levels in lysed cells. WT or TTL KO MEFs were lysed in a Triton X-100–based buffer, taxol stabilized, fixed, and labeled with tyrosinated (Tyr) and detyrosinated (Detyr) tubulin antibodies. WT + CPA indicates WT lysed MEFs incubated with CPA before fixation. (B) MCAK effects on lysed cells. Images of MT arrays under control conditions or after exposure to recombinant full-length MCAK. (C) Quantitative analysis of MT depolymerization in the presence of full-length MCAK or MCAK domains. The MT signal is the percentage \pm SEM of the area occupied by the MT network versus total cell area. A minimum of 78 lysed cells was analyzed in each condition. ***, $P < 0.001$ with a t test. Bars, 50 μ m.

neurons display morphogenetic anomalies affecting axonal length and branching (Homma et al., 2003). In an analysis of TTL KO neurons morphology, we observed an increase in both the axon length and the total length of axon collaterals. The number of primary collaterals per unit of axonal length was unaffected, whereas the total number of collaterals, including secondary or tertiary branches, was increased (Fig. 5, D–G). These anomalies resemble those observed in KIF2A KO neurons (Homma et al., 2003). Collectively, our data strongly suggest that KIF2A activity is inhibited in TTL KO neurons, and this is supported by experiments in lysed MEFs showing inhibited KIF2A activity on WT CPA or TTL KO MTs compared with WT polymer (Fig. 5 H).

The influence of the tubulin tyrosination status on the activity of depolymerizing motors provides an elegant mechanistic explanation for the observed stability of detyrosinated MTs. Tubulin tyrosination affects the activity of the neck + motor mutant of MCAK, which lacks both the N-terminal and C-terminal domains of MCAK. This suggests that neither domain is centrally involved in MCAK interactions with the tubulin C terminus. Both of these domains are implicated in MCAK's ability to track on MT ends, which has been shown to be unaffected by tubulin detyrosination (Moore et al., 2005; Peris et al., 2006). Based on our data, MT detyrosination negatively affects MCAK's tubulin removal activity directly. Thus, tubulin detyrosination, and its negative effect on kinesin-13 family motors, is the most likely explanation for

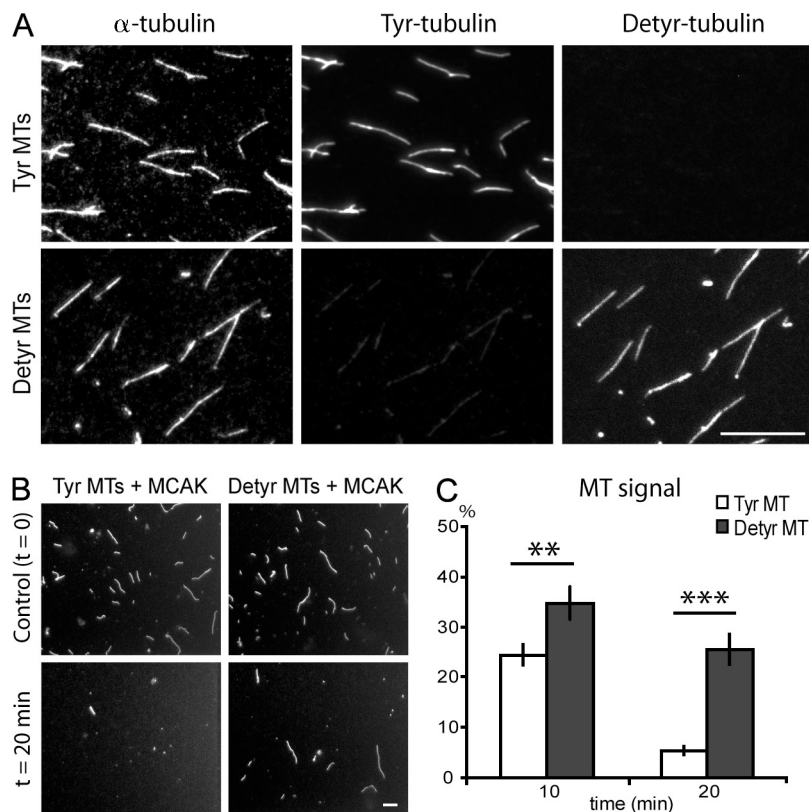


Figure 3. Depolymerizing activity of MCAK on pure tyrosinated or detyrosinated MTs. (A) Tyrosinated (Tyr) and detyrosinated (Detyr) MTs stained for either total, tyrosinated, or detyrosinated tubulin. (B) Representative pictures of tyrosinated and detyrosinated MT before and after exposure to MCAK for 20 min. (C) Analysis of MT depolymerization in the presence of MCAK. The MT signal is the percentage \pm SEM of the area occupied by the MT at time 10 or 20 min versus time 0. A minimum of 20 independent images was measured in each condition. **, $P < 0.01$; and ***, $P < 0.001$ with a t test. Bars, 10 μ m.

the impairment of MT disassembly observed in TTL KO cells. A contribution of other modifications of the tubulin C terminus such as polyglutamylation, which could be affected by detyrosination and resulting MT stabilization, cannot be completely ruled out, but polyglutamylation is minimal in cycling cells.

Our results suggest a direct role for tubulin detyrosination in MCAK inhibition and invalidate an indirect effect through CAP-Gly + tip-interacting protein (TIP) delocalization in TTL KO cells. Indeed, although MT detyrosination impairs CAP-Gly + TIP localization at plus ends (Peris et al., 2006), this delocalization of CAP-Gly + TIP from MT ends induces a decrease in the rescue frequency and premature MT catastrophes close to membranes (Komarova et al., 2002). In contrast, we observed the opposite MT dynamic parameters in TTL KO cells. Thus, we cannot attribute the increased MT stability to the absence of CAP-Gly + TIP at MT plus ends.

The ADP-Pi- or ADP-bound forms of MCAK associate less efficiently with detyrosinated than with tyrosinated MTs, suggesting that the lattice dwell time for MCAK between cycles of hydrolysis is lower on detyrosinated than on tyrosinated MTs. This would substantially decrease the number of tubulin dimers removed per motor before detaching from the MT (Helenius et al., 2006; Wagenbach et al., 2008). It would also limit the ability of MCAK to find MT ends by diffusive motility (Helenius et al., 2006). In current models, the ADP-Pi or ADP forms of MCAK are retained in the vicinity of the MT lattice through weak electrostatic interaction with the charged E-hook of the α -tubulin C terminus (Helenius et al., 2006). Our data demonstrate an important regulatory role for the C-terminal Tyr of α -tubulin in the autoregulation of MT stability.

Impaired MT disassembly has been previously observed in KIF2A-deficient neurons (Homma et al., 2003) or upon MCAK inhibition in cycling cells (Mennella et al., 2005). Obviously, kinesin-13 inhibition provides a highly plausible explanation for the impaired MT disassembly observed in different TTL KO cell types in this study. Additionally, MCAK appears to be important for MT disassembly upon encountering the cell edge, and may be crucial for end-on attachments to specific membrane complexes (Geiger et al., 1984; Morrison, 2007).

Impaired activity of depolymerizing motors may be central to several anomalies observed in TTL KO cells or mice. There is extensive overlap between the phenotypes observed in TTL KO or KIF2A KO neurons or mice (Homma et al., 2003; Erck et al., 2005). Anomalies and adaptations in depolymerizing motor activity may also be important for the facilitating effect of TTL loss on tumor progression (Mialhe et al., 2001). MCAK activity has been observed to be altered in cancer cells (Hedrick et al., 2008; Ishikawa et al., 2008). Interestingly, both CAP-Gly plus end-binding proteins and depolymerizing motors have been identified as factors whose alteration favors genomic instability in aneuploid cells and thus malignant cell invasiveness (Storchova et al., 2006; Pellman, 2007).

Factors able to promote the differentiation of cellular MTs into distinct stability subclasses have been the subject of sustained interest in cell biology. Decades ago, tubulin tyrosination, which distinguished with striking clarity between stable and dynamic MTs, seemed to be an ideal mechanism responsible for selective MT stabilization (Schulze et al., 1987). This attractive view was discarded when it appeared that tyrosination

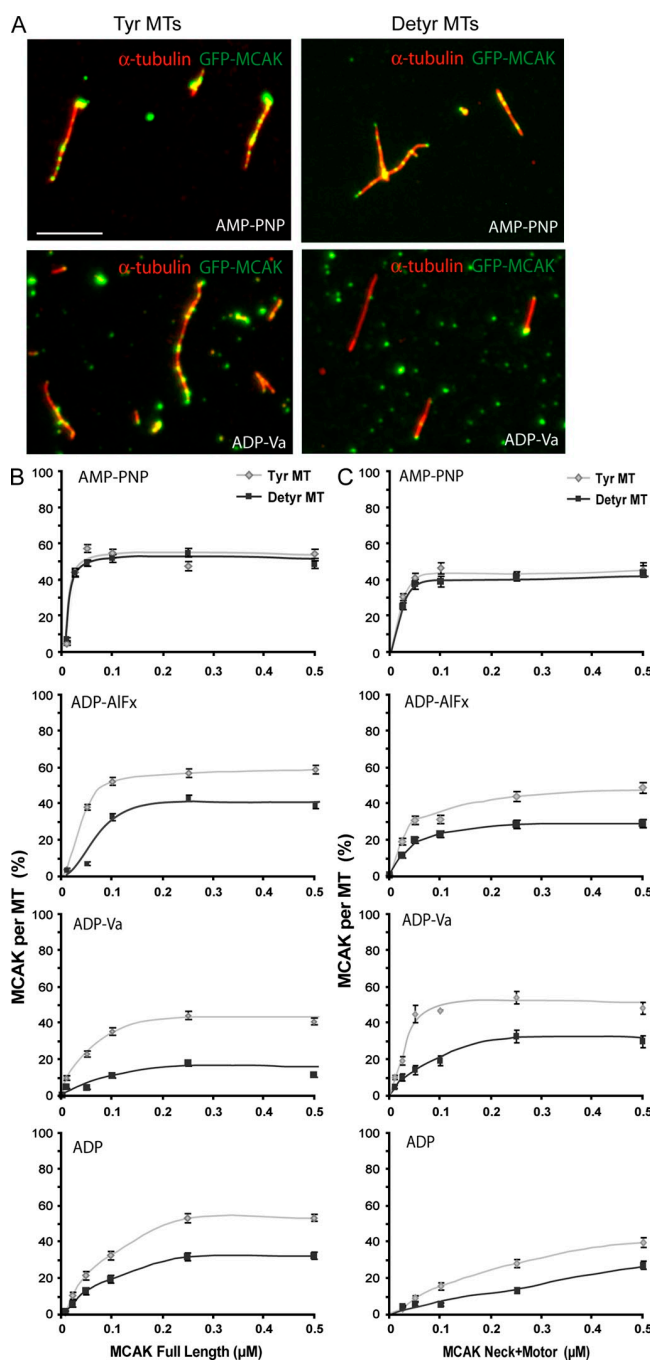


Figure 4. Tubulin tyrosination affects the interaction of MCAK with MTs. (A) Fluorescence images of MCAK binding to MTs. Equal amounts of taxol-stabilized (10 nM) tyrosinated (Tyr) or detyrosinated (Detyr) pure tubulin MTs (red) were incubated with 0.25 μ M purified GFP-MCAK (green) in AMP-PNP- or ADP-vanadate (Va)-bound forms. (B and C) Quantitative analysis of full-length MCAK (B) or MCAK neck + motor domain (C) association with equal amounts (10 nM) of pure Tyr or Glu MTs at different motor concentrations and in the presence of various nucleotides. Motor binding was measured as the ratio of the motor signal versus MT signal (MCAK per MT %). Mean \pm SEM. At least 100 MTs were analyzed for each condition. Bar, 5 μ m.

does not, per se, alter MT dynamic properties. Based on our results, tubulin detyrosination could actually generate persistent stable MT subsets by rendering transiently stabilized MTs resistant to motor-driven depolymerization.

Materials and methods

Antibodies

The antibodies used were detyrosinated tubulin (L4), tyrosinated tubulin (clone YL1/2), α -tubulin (clone α 3a; Peris et al., 2006), polyclonal anti-GFP (Invitrogen), and polyclonal anti-MCAK (Andrews et al., 2004).

Cell culture and transfection

Hippocampal neurons and MEFs (three different embryos for each genotype) were prepared as previously described (Erck et al., 2005). MEFs were transfected using MEF Nucleofector kits (Amaya Biosystems) and GFP-EB3 (provided by N. Galjart, Erasmus Medical Center, Rotterdam, Netherlands), m-cherry α -tubulin (provided by F. Saudou, Institut Curie, Paris, France), and m-cherry-MCAK (Wordeman laboratory). For inhibition of MCAK, Stealth siRNA Negative Control, Stealth Select siRNA 1 MSS232130, siRNA 2 MSS232131, and siRNA 3 MSS232132 (all from Invitrogen) were used. MCAK inhibition was assayed by Western blot analysis, and siRNA 3 was used in MT dynamic analysis.

Recombinant proteins

The His₆-tagged HsKIF2A neck + motor domain (residues 188–537) was expressed in the BL21 bacterial strain. His₆-tagged full-length MCAK, MCAK₁₈₂₋₅₈₃, and EGFP-MCAK₁₈₂₋₅₈₃ were expressed in baculovirus.

Nocodazole susceptibility assay

Cells were treated with carrier alone or with 20 μ M nocodazole for 60 min (neurons) or 15 min (MEFs), permeabilized in PHEM buffer (60 mM Pipes, 25 mM Hepes, 10 mM EGTA, and 2 mM MgCl₂, pH 6.9) with 0.02% saponin and 10 μ M taxol, and fixed in PHEM buffer with 2% paraformaldehyde and 0.05% glutaraldehyde. The MT network was quantified by the α -tubulin fluorescence intensity measured inside the whole cell surface in fibroblasts (determined with F-actin staining) or in three fixed size regions (5 \times 5 μ m) placed at the proximal, medial, and distal part of each axon.

Immunofluorescence and video microscopy

Fluorescent images of living cells were captured with a charge-coupled device camera (CoolSNAP HQ; Roper Scientific) using a 100 \times NA 1.3 Plan-Neofluar oil objective in an inverted motorized microscope (Axiovert 200M; Carl Zeiss, Inc.) controlled by MetaMorph software (MDS Analytical Technologies). Fixed images were captured with a charge-coupled device camera (CoolSNAP ES; Roper Scientific) in a straight microscope (Axioskop 50; Carl Zeiss, Inc.) controlled by MetaView software (MDS Analytical Technologies) using a 40 \times or 100 \times NA 1.3 Plan-Neofluar oil objective.

Analysis of MT behavior

Image capture was every 3 s. MTs displaying a trajectory at a straight angle (70–110°) with the cell membrane were analyzed inside a region of 10 μ m from the cell edge. MT persistence time, measured for polymers whose growing end made contact with the membrane, was defined as the time during which at least a segment of MT kept running parallel to the membrane before disassembly. MT dynamic instability parameters were determined and analyzed as previously described (Kline-Smith and Walczak, 2002).

Lysed cell experiments

Fibroblasts were lysed in PEM buffer (80 mM Pipes, 1 mM EGTA, and 1 mM MgCl₂, pH 6.7) with 0.5% Triton X-100 and 10% glycerol and incubated in PEM with 2 μ M of taxol buffer in the presence or absence of 2 μ g/ml CPA (Sigma-Aldrich). Lysed cells were then washed in CPA-inactivating buffer (20 mM DDT in PEM-taxol buffer) and extensively washed in PEM-taxol buffer. Lysed cells were incubated with buffer alone (PEM buffer, 2 μ M taxol, 1 mM DTT, 75 mM KCl, and 0.25 mM Mg-ATP) or with the same buffer containing purified motor protein (200 nM for MCAK proteins and 800 nM for KIF2A) for 30 min and then fixed in cold methanol. The MT network was quantified by the α -tubulin fluorescence intensity measured inside the whole cell surface of lysed cells.

Motor binding to MTs

Motor binding to MTs was assayed in different nucleotide conditions: AMP-PNP, ADP-aluminum fluoride, ADP-vanadate, and ADP. 1 μ M of purified motors was incubated with 2 mM of nucleotides and then with 0.01 μ M of tyrosinated or detyrosinated taxol-stabilized MTs (Paturle et al., 1989). Reactions were stopped with PEM, 50% glycerol, and 1% glutaraldehyde and centrifuged on coverslips. MT-motor complexes were fixed in cold methanol and double stained with α -tubulin and GFP antibodies. For quantification,

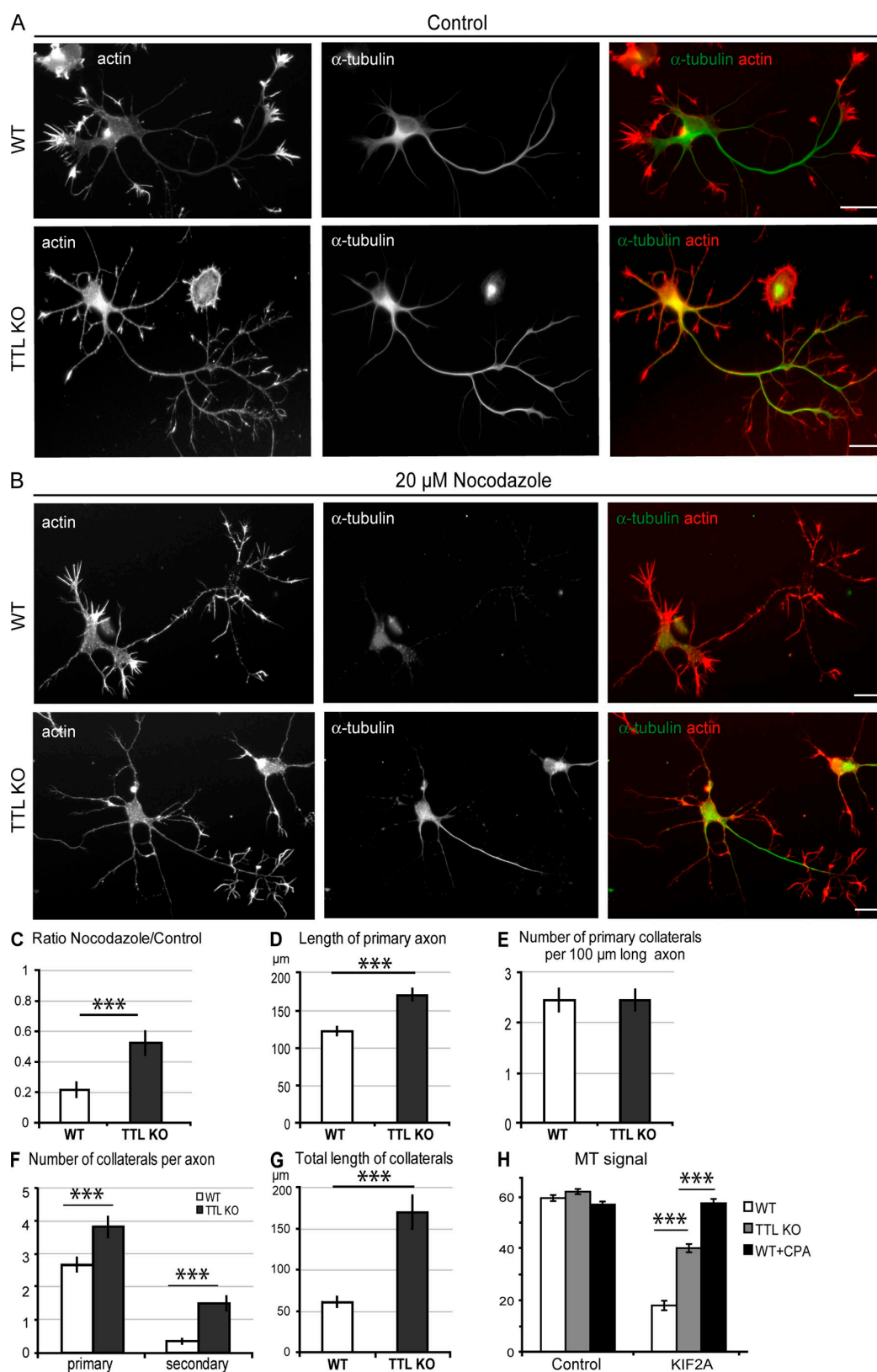


Figure 5. Impaired MT disassembly and abnormal cell morphology in TTL KO-cultured neurons. (A and B) WT or TTL KO hippocampal neurons 2 d after plating. Neurons were incubated in the absence (control; A) or presence of 20 μ M nocodazole (B), permeabilized in saponin-based buffer to extract free tubulin molecules, and double labeled for F-actin (red) and tubulin (green). (C) Quantitative analysis of nocodazole effects. The axonal MT signal was expressed as the ratio of MT signals measured after nocodazole treatment versus control conditions (mean values \pm SEM). MT signals were estimated for a minimum of 50 axons from three independent experiments. (D–G) Cell morphology in WT or TTL KO neurons showing length, number of primary or of higher order collaterals, and total length of collaterals. Mean values \pm SEM for 93 WT neurons and 123 TTL KO neurons from three independent experiments are shown. (H) Depolymerizing activity of the neck + motor construct of KIF2A on tyrosinated or detyrosinated MTs. The assay was performed as in Fig. 2 C. Mean values \pm SEM for 75 cells are shown. ***, $P < 0.001$ with a t test. Bars, 20 μ m.

a line corresponding to each MT in the α -tubulin image was transferred to the GFP images. The amount of motor bound per unit of MT length was calculated as the percentage of positive GFP pixels versus the total number of pixels in the MT line.

In vitro depolymerization experiments

10 nM of taxol-stabilized tyrosinated or detyrosinated MTs were or were not incubated with 10 nM MCAK-ATP. Reactions were stopped with PEM, 50% glycerol, and 1% glutaraldehyde after 10 or 20 min and centrifuged on coverslips. Reactions were fixed in cold methanol and stained with anti-tubulin antibody. Quantification of the total amount of MTs was measured using ImageJ software (National Institutes of Health).

Data processing and analysis

Data were analyzed blind to the genotype or the experimental conditions. For statistical analysis, *t* tests with unequal variances for samples comprising >30 measures or a parametric Mann and Whitney *U* test for smaller samples was used.

Online supplemental material

Fig. S1 illustrates endogenous MCAK expression in WT or TTL KO MEFs and its specific suppression with commercial Stealth siRNAs. Fig. S2 represents life history plots of individual MTs from WT or TTL MEFs with endogenous levels or overexpression or suppression of MCAK. Videos 1 and 2 show time-lapse video microscopy of a lamellipodial extension of a WT and TTL KO fibroblast, respectively, expressing m-cherry α -tubulin and GFP-EB3. Videos 3 and 4 show time-lapse video microscopy of a lamellipodial extension of a WT and TTL KO fibroblast, respectively, expressing m-cherry MCAK and GFP-EB3. Videos 5 and 6 show time-lapse video microscopy of a lamellipodial extension of a WT and TTL KO fibroblast, respectively, treated with MCAK siRNA for 36 h and expressing m-cherry α -tubulin and GFP-EB3. Online supplemental material is available at <http://www.jcb.org/cgi/content/full/jcb.200902142/DC1>.

We thank A. Andrieux's team members for comments on the manuscript and D. Proietto, A. Schweitzer, J.P. Andrieu, and B. Dublet for technical help.

This work was supported in part by grants from the Agence Nationale de la Recherche Tyr-Tips to D. Job, la Ligue contre le cancer to D. Job, the Association Recherche sur le Cancer to D. Job and A. Andrieu, and the National Institutes of Health (GM069429) to L. Wordeman.

Submitted: 26 February 2009

Accepted: 2 June 2009

References

- Andrews, P.D., Y. Ovechkina, N. Morrice, M. Wagenbach, K. Duncan, L. Wordeman, and J.R. Swedlow. 2004. Aurora B regulates MCAK at the mitotic centromere. *Dev. Cell.* 6:253–268.
- Badin-Larcon, A.C., C. Boscheron, J.M. Soleilhac, M. Piel, C. Mann, E. Denarier, A. Fourest-Lieuvin, L. Lafanechère, M. Bornens, and D. Job. 2004. Suppression of nuclear oscillations in *Saccharomyces cerevisiae* expressing Glu tubulin. *Proc. Natl. Acad. Sci. USA.* 101:5577–5582.
- Bieling, P., S. Kandels-Lewis, I.A. Telley, J. van Dijk, C. Janke, and T. Surrey. 2008. CLIP-170 tracks growing microtubule ends by dynamically recognizing composite EB1/tubulin-binding sites. *J. Cell Biol.* 183:1223–1233.
- Erck, C., L. Peris, A. Andrieux, C. Meissirel, A.D. Gruber, M. Vernet, A. Schweitzer, Y. Saoudi, H. Pointu, C. Bosc, et al. 2005. A vital role of tubulin-tyrosine-ligase for neuronal organization. *Proc. Natl. Acad. Sci. USA.* 102:7853–7858.
- Geiger, B., Z. Avnur, G. Rinnerthaler, H. Hinssen, and V.J. Small. 1984. Microfilament-organizing centers in areas of cell contact: cytoskeletal interactions during cell attachment and locomotion. *J. Cell Biol.* 99:83s–91s.
- Gupta, M.L. Jr., P. Carvalho, D.M. Roof, and D. Pellman. 2006. Plus end-specific depolymerase activity of Kip3, a kinesin-8 protein, explains its role in positioning the yeast mitotic spindle. *Nat. Cell Biol.* 8:913–923.
- Hammond, J.W., D. Cai, and K.J. Verhey. 2008. Tubulin modifications and their cellular functions. *Curr. Opin. Cell Biol.* 20:71–76.
- Hedrick, D.G., J.R. Stout, and C.E. Walczak. 2008. Effects of anti-microtubule agents on microtubule organization in cells lacking the kinesin-13 MCAK. *Cell Cycle.* 7:2146–2156.
- Helenius, J., G. Brouhard, Y. Kalaidzidis, S. Diez, and J. Howard. 2006. The depolymerizing kinesin MCAK uses lattice diffusion to rapidly target microtubule ends. *Nature.* 441:115–119.
- Homma, N., Y. Takei, Y. Tanaka, T. Nakata, S. Terada, M. Kikkawa, Y. Noda, and N. Hirokawa. 2003. Kinesin superfamily protein 2A (KIF2A) functions in suppression of collateral branch extension. *Cell.* 114:229–239.
- Ishikawa, K., Y. Kamohara, F. Tanaka, N. Haraguchi, K. Mimori, H. Inoue, and M. Mori. 2008. Mitotic centromere-associated kinesin is a novel marker for prognosis and lymph node metastasis in colorectal cancer. *Br. J. Cancer.* 98:1824–1829.
- Khawaja, S., G.G. Gundersen, and J.C. Bulinski. 1988. Enhanced stability of microtubules enriched in detyrosinated tubulin is not a direct function of detyrosination level. *J. Cell Biol.* 106:141–149.
- Kline-Smith, S.L., and C.E. Walczak. 2002. The microtubule-destabilizing kinesin XKCM1 regulates microtubule dynamic instability in cells. *Mol. Biol. Cell.* 13:2718–2731.
- Komarova, Y.A., A.S. Akhmanova, S. Kojima, N. Galjart, and G.G. Borisy. 2002. Cytoplasmic linker proteins promote microtubule rescue in vivo. *J. Cell Biol.* 159:589–599.
- Maney, T., M. Wagenbach, and L. Wordeman. 2001. Molecular dissection of the microtubule depolymerizing activity of mitotic centromere-associated kinesin. *J. Biol. Chem.* 276:34753–34758.
- Manning, A.L., N.J. Ganem, S.F. Bakhom, M. Wagenbach, L. Wordeman, and D.A. Compton. 2007. The kinesin-13 proteins Kif2a, Kif2b, and Kif2c/MCAK have distinct roles during mitosis in human cells. *Mol. Biol. Cell.* 18:2970–2979.
- Mennella, V., G.C. Rogers, S.L. Rogers, D.W. Buster, R.D. Vale, and D.J. Sharp. 2005. Functionally distinct kinesin-13 family members cooperate to regulate microtubule dynamics during interphase. *Nat. Cell Biol.* 7:235–245.
- Mialhe, A., L. Lafanechère, I. Treilleux, N. Peloux, C. Dumontet, A. Bremond, M.H. Panh, R. Payan, J. Wehland, R.L. Margolis, and D. Job. 2001. Tubulin detyrosination is a frequent occurrence in breast cancers of poor prognosis. *Cancer Res.* 61:5024–5027.
- Moore, A., and L. Wordeman. 2004. C-terminus of mitotic centromere-associated kinesin (MCAK) inhibits its lattice-stimulated ATPase activity. *Biochem. J.* 383:227–235.
- Moore, A.T., K.E. Rankin, G. von Dassow, L. Peris, M. Wagenbach, Y. Ovechkina, A. Andrieux, D. Job, and L. Wordeman. 2005. MCAK associates with the tips of polymerizing microtubules. *J. Cell Biol.* 169:391–397.
- Morrison, E.E. 2007. Action and interactions at microtubule ends. *Cell. Mol. Life Sci.* 64:307–317.
- Newton, C.N., M. Wagenbach, Y. Ovechkina, L. Wordeman, and L. Wilson. 2004. MCAK, a Kin I kinesin, increases the catastrophe frequency of steady-state HeLa cell microtubules in an ATP-dependent manner in vitro. *FEBS Lett.* 572:80–84.
- Ohi, R., K. Burbank, Q. Liu, and T.J. Mitchison. 2007. Nonredundant functions of Kinesin-13s during meiotic spindle assembly. *Curr. Biol.* 17:953–959.
- Paturle, L., J. Wehland, R.L. Margolis, and D. Job. 1989. Complete separation of tyrosinated, detyrosinated, and nontyrosinatable brain tubulin subpopulations using affinity chromatography. *Biochemistry.* 28:2698–2704.
- Pellman, D. 2007. Cell biology: aneuploidy and cancer. *Nature.* 446:38–39.
- Peris, L., M. Thery, J. Fauré, Y. Saoudi, L. Lafanechère, J.K. Chilton, P. Gordon-Weeks, N. Galjart, M. Bornens, L. Wordeman, et al. 2006. Tubulin tyrosination is a major factor affecting the recruitment of CAP-Gly proteins at microtubule plus ends. *J. Cell Biol.* 174:839–849.
- Saoudi, Y., I. Paintrand, L. Multigner, and D. Job. 1995. Stabilization and bundling of subtilisin-treated microtubules induced by microtubule associated proteins. *J. Cell Sci.* 108:357–367.
- Schulze, E., D.J. Asai, J.C. Bulinski, and M. Kirschner. 1987. Posttranslational modification and microtubule stability. *J. Cell Biol.* 105:2167–2177.
- Steinmetz, M.O., and A. Akhmanova. 2008. Capturing protein tails by CAP-Gly domains. *Trends Biochem. Sci.* 33:535–545.
- Storchova, Z., A. Breneman, J. Cande, J. Dunn, K. Burbank, E. O'Toole, and D. Pellman. 2006. Genome-wide genetic analysis of polyploidy in yeast. *Nature.* 443:541–547.
- Wagenbach, M., S. Domnitz, L. Wordeman, and J. Cooper. 2008. A kinesin-13 mutant catalytically depolymerizes microtubules in ADP. *J. Cell Biol.* 183:617–623.
- Webster, D.R., G.G. Gundersen, J.C. Bulinski, and G.G. Borisy. 1987. Assembly and turnover of detyrosinated tubulin in vivo. *J. Cell Biol.* 105:265–276.